Front. Optoelectron. 2012, 5(1): 68–72
DOI 10.1007/s12200-012-0195-8

RESEARCH ARTICLE

Energy intensity analysis of modes in hybrid plasmonic waveguide

Ruixi ZENG[1,2], Yuan ZHANG (✉)[1], Sailing HE[1,2]

1 Centre for Optical and Electromagnetic Research, State Key Laboratory of Modern Optical Instrumentations, Zhejiang University, Hangzhou 310058, China
2 Joint Research Center of Photonics of Zhejiang University and South China Normal University, South China Normal University, Guangzhou 510006, China

Abstract A hybrid plasmonic waveguide containing silicon core, silver cap and ultra-thin sandwiched SiO_2 layer is studied. By analyzing the mode distribution patterns and the curves of mode effective index, we show how the plasmonic mode around the metal surface is coupled with the fundamental mode in the silicon core to form a squeezed hybrid mode. The ability of the hybrid plasmonic waveguide in energy confinement is also discussed quantitatively.

Keywords plasmonic, hybrid plasmonic waveguide, energy intensity, integration density

1 Introduction

With the ability to confine optical modes better than dielectric waveguides, plasmonic waveguides [1,2] have attracted much interest during the past decade. Much work [3–9] has been done to improve the performance and integration density of photonic circuits. Although the plasmonic waveguide can work beyond the so-called “diffraction limit”, there is always a key obstacle, that is, a tradeoff between the mode confinement and the mode loss. To overcome such a drawback, hybrid plasmonic waveguides have been introduced quite recently, and several hybrid designs have been proposed [10–15]. The main feature of this kind of designs is one extreme thin (around or even thinner than 10 nm) low index layer sandwiched by thick high index strip (or cylinder) and metal substrate (or cap). In such a special structure, the main part of the mode energy is squeezed into the thin low index layer, and thus we can get a deep sub-wavelength optical mode with acceptable mode loss. In this paper, we examine some detail issues of the hybrid plasmonic waveguide to understand how the optical mode changes with the physical geometry, and discuss its ability to confine light.

2 Geometry parameters of hybrid plasmonic waveguide

Geometries of hybrid plasmonic waveguides studied in this paper are shown in Fig. 1. With consideration to the fabrication convenience, here we choose two types of hybrid structures, which can be made by different lift-off and etching processes. In Fig. 1, the silicon core has a height of h_{Si} and a width of w_2; we use silver (Ag) as the top metal cap with width w_1 and height h_m; structure (a) can be obtained from (b) by etching the SiO_2 layer using the top silver strip as a mask. Both hybrid structures can be fabricated based on silicon-on-insulator (SOI) chips, which have an insulator buffer layer on the high index silicon substrate. However, we do not include them in our simulations for simplicity to discuss the hybrid plasmonic mode properties, i.e., we assume that the hybrid structures are surrounded by air as shown in Fig. 1. The working wavelength studied in this paper is set to 1550 nm and the permittivity of the Ag cap is $0.1453 + 11.3567i$ [16]. In the design of Fig. 1, we set $h_{SiO_2} = 20$ nm, $h_m = 100$ nm and $h_{Si} = 400$ nm.

3 Hybrid plasmonic mode analysis

In this paper, we are interested in the fundamental modes of the hybrid plasmonic waveguides, and the higher order modes are not considered when w_2 is optically large. At first, we study the effective index (n_{eff}) of the two structures in Fig. 1. As there is a lossy metal in the

Received September 29, 2011; accepted November 15, 2011

E-mail: zhydxx@zju.edu.cn

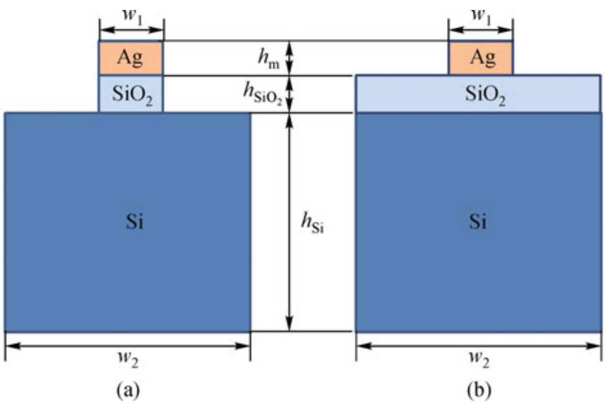

Fig. 1 Cross section of the two hybrid plasmonic waveguides studied in this paper

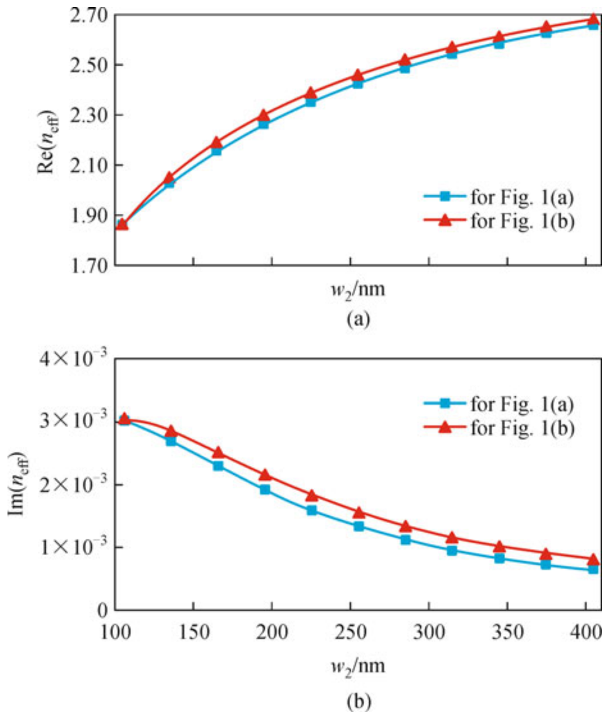

Fig. 2 Real part (a) and imaginary part (b) of effective index of the two types of designs in Fig. 1 as the width of the silicon core increases. Blue square curves and red triangle curves are for structures in Figs. 1(a) and 1(b), respectively

structure, the effective index is a complex value. We can estimate the mode propagating length (L) by the imaginary part of the effective index through $L = 1/(\mathrm{Im}(n_{\mathrm{eff}}) \times k_0)$, where k_0 is the wave vector in vacuum ($k_0 = 2\pi/\lambda$). By definition, the propagating energy will be only 1/e of the original input energy after propagating over a length of L. In Fig. 2, the blue square curve and red triangle curve are for Figs. 1(a) and 1(b) when w_2 varies from 100 to 400 nm, respectively. From Fig. 2, we can see that both curves are quite close to each other, which means the width of SiO_2 do not affect much the mode effective index. The reason is that the SiO_2 layer is very thin, and the area not covered by the Ag cap does not contain much electromagnetic (EM) field. Actually our simulation results have shown that the distributions of the modal fields for the two kinds of design in Fig. 1 are quite similar. Thus we will focus on the structure of Fig. 1(a) to study the details of the energy distribution of the plasmonic modes.

For clarity, we show the energy flux density distribution for the modes with w_2 = 100, 200, and 400 nm in Figs. 3(a) to 3(c), respectively. The black curve shows the energy flux density distribution along the white midline in each figure, and the sharp peaks indicate the deep sub-wavelength field confinement in y direction just like that in Ref. [10]. The mode distributions indicate that some part of energy has been squeezed into the SiO_2 gaps, which make a bright spot in these figures. For Fig. 3(a), if we consider the silicon core independently, there is no fundamental mode for the pure silicon waveguide, which makes the EM energy decay exponentially (see the tail of the curve) in the silicon core. Thus the surface mode of the metal cap is dominant in this case. As the width of the silicon core increases to 200 nm (see Fig. 3(b)), more energy will be grabbed by the silicon core, which causes a slowly growing peak in the cross section curve (and the color in the Si part is slightly brighter than Fig. 3(a)). When the width of the silicon core increases further to 400 nm, more and more energy is dragged into the silicon (see the bright spot in Fig. 3(c)), which can also be checked in the curve along the cross line. This is because a 400 nm×400 nm silicon waveguide can support a fundamental mode very well, and the silicon waveguide mode takes more part of the energy than the SiO_2 gap. The patterns from Figs. 3(a) to 3(c) show a clear trend how the pure plasmonic mode interacts with the pure dielectric waveguide mode. Taking w_2 = 200 nm for example, as shown in Fig. 3(d), the hybrid palsmonic mode can be explained by the coupling of a plasmonic mode of the metal cap and the waveguide mode of a pure dielectric waveguide.

We also check the waveguide property when the width of the metal cap varies while the width of the silicon core keeps constant. Taking the design in Fig. 1(a) for example, geometry parameters are set to h_{Si} = 250 nm, $h_{\mathrm{SiO_2}}$ = 20 nm and h_{m} = 100 nm. When the metal cap width is changing, for comparison, we choose two different silicon core width w_2 = 400 and 200 nm. The silicon core can support the fundamental mode for w_2 = 400 nm, but not for w_2 = 200 nm. The curves of both real and imaginary parts of the effective index are shown in Fig. 4. We can see that both structures have the same trend of effective index variation as w_1 increases. Combining with Fig. 3, we can understand that as the silicon core gets broader, more EM field will stay in the high index core, which makes the real part of n_{eff} in Fig. 4(a) larger than that in Fig. 4(b). The interesting

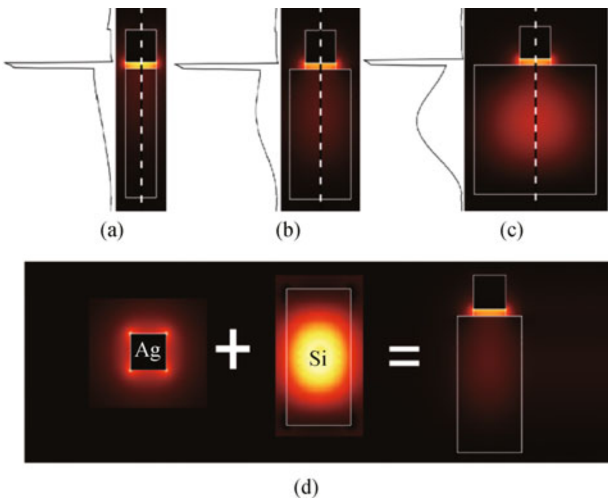

Fig. 3 Energy flux density distributions of hybrid plasmonic mode for structure of Fig. 1(a) when silicon width is (a) 100 nm; (b) 200 nm; and (c) 400 nm. Black curve at the left of each pattern is the distribution along the cross section (dashed lines); (d) illustration showing plasmonic mode and dielectric mode couple to form a hybrid plasmonic waveguide mode

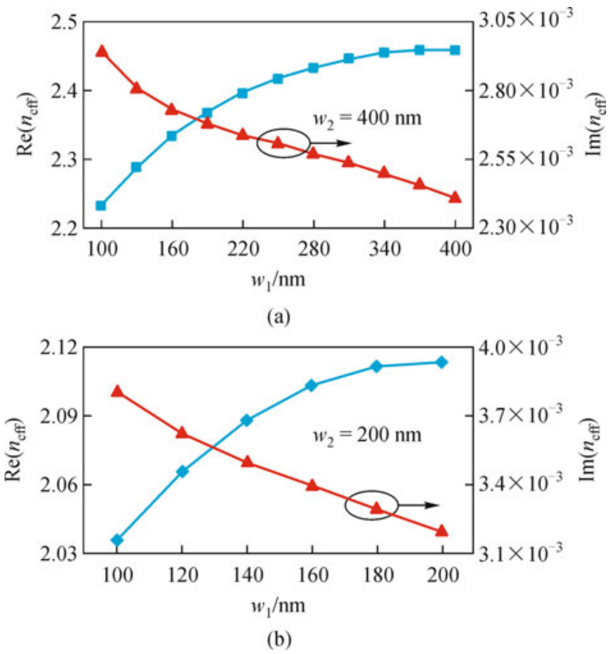

Fig. 4 Real part (blue curve) and imaginary part (red curve) of effective index as the width of metal cap increases when the width of silicon core is fixed to (a) 400 nm; and (b) 200 nm (h_{Si} = 250 nm, h_{SiO_2} = 20 nm; h_m = 100 nm)

thing is the imaginary part of n_{eff}. When the metal cap shrinks, the overlap of the EM field and the metal cap decreases, which means a lower loss caused by the metal absorption. However, we found the opposite results in Fig. 4, i.e., when the metal cap shrinks the mode loss increases. This is because when the metal size gets smaller, the radiation effect will become stronger, and this additional radiation mode loss cannot be compensated by the reduction of the metal absorption. Thus, we should also consider the radiation loss in the mode besides the metal absorption loss. As a result, we get a larger imaginary part of n_{eff} as the metal cap becomes smaller.

4 Energy confinement in hybrid plasmonic waveguide

The purpose of using plasmonic structures in optical waveguides is to shrink the optical mode size. One advantage of a hybrid plasmonic waveguide is that the mode size can be squeezed even to several nanometers. From the discussion in the above sections, it can be seen that the highly confined mode is mainly located in the very thin SiO_2 layer. Therefore, it is necessary to study how the EM energy is stored in such a hybrid plasmonic waveguide. As people are more interested in the energy stored in and around the gap layer (the SiO_2 layer in this paper), here we define a special hybrid plasmonic mode size (S_{gmode}) as the area included by the contour of ξ in the two-dimensional time-averaged energy flow distribution (where ξ is defined as $1/e^2$ of the maximum value of the time-averaged energy flow distribution in the SiO_2 layer); and the energy stored in this area as E_{gmode}. E_{gmode} can be used to estimate the energy stored in and around the SiO_2 layer in two-dimensional time-averaged energy flow distribution (as those in Figs. 3(a)–3(c)). For some cases with large w_2 , the energy flux in some part of the Si core may be larger than ξ (as the case in Fig. 3(c)), which indicates that this area in Si should be included in the area of S_{gmode}. However, we do not include any area in Si to S_{gmode}, since we are more interested in the energy distribution in the SiO_2 layer. We still take the structure in Fig. 1(a) for example, and the geometry parameters are w_1 = 100 nm, h_m = 100 nm, h_{SiO_2} = 20 nm, h_{Si} = 400 nm, and w_2 varies from 100 to 400 nm. Our computation (not shown here) indicates that S_{gmode} is not affected much by the silicon core width, and the mode size is very close to the value of SiO_2 area. To evaluate the energy confinement ability of the optical mode in our hybrid plasmonic waveguide, we define a confinement factor C_{gmode} as

$$C_{gmode} = E_{gmode}/E_{total}, \quad (1)$$

where E_{total} stands for the energy of the whole optical mode.

In Fig. 5, we plot the relationship between the confinement factor C_{gmode} and w_2 (from 100 to 400 nm) in red curve (corresponding to the blue square curves in Fig. 2). This confinement factor gives the estimated ratio of energy in area of S_{gmode} to the total mode energy. We can see that the energy in the highly confined area decreases as w_2 increases. When w_2 = 400 nm, C_{gmode} is about 0.1, and

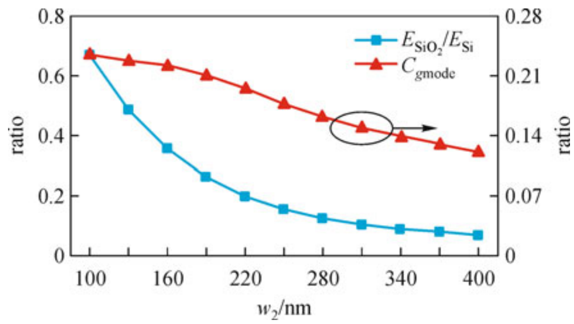

Fig. 5 Confinement factor C_{gmode} (red triangle curve) and the ratio of energy stored in SiO_2 to that in Si core (blue square curve) as w_2 increases from 100 to 400 nm

the highest value of C_{gmode} is limited to 0.25 when w_2 = 100 nm. This means most parts of energy are not in the SiO_2 layer. This is quite different from normal optical mode, where most mode energy is in its own S_{gmode}. In the purpose of finding the reason, we should go back to check the mode energy distributions in Fig. 3. We can see that the total mode energy can be divided into three parts: one part is stored in and around the SiO_2 layer, one part mainly in and around the silicon core, and the last part is the energy around the metal cap (except those in the SiO_2 layer). Actually, the third part contains considerable energy, because the EM field can go around the silver cap by side coupling (through some surface plasmon waves). We can also make a rough estimation from the cross section distribution in Fig. 3. The sharp peak around the SiO_2 layer comes from the discontinuity of E_y at different index material boundaries, which makes the energy density quite high in the SiO_2 layer (see those bright hot spots in Fig. 3). However, this cannot lead to a large energy confinement in the area of S_{gmode}, since the sharp peak grows quickly along the high/low index boundary, which makes the value of ξ quite high. Thus, most energy is excluded from the area of S_{gmode}, and this excluded part of energy is large in total although with low energy density. That is, if we compare the integral over the SiO_2 layer region and the total integral over the whole region, we can see that the former one is quite small, just occupying a small percentage of the total energy. Therefore, the hybrid plasmonic waveguide is good for high energy density, rather than real energy confinement. The blue curve in Fig. 5 shows the proportion of E_{SiO_2} to E_{Si}, where E_{SiO_2} and E_{Si} are the energy stored in SiO_2 layer and silicon core, respectively. Even the energy stored in the silicon core is much larger than that in the SiO_2 layer.

5 Conclusions

In conclusion, we have studied some optical mode properties of a hybrid plasmonic waveguide in this paper. We have shown how the effective index of the modes changes as the physical geometry varies. By plotting the mode patterns, we have shown how a plasmonic mode and a pure fundamental dielectric mode are coupled to form a hybrid plasmonic mode with deep sub-wavelength mode size. We have also studied the energy confinement of such a hybrid plasmonic mode, and found that the energy stored in the highly squeezed mode (energy in the area enclosed by the ξ contour) is quite small although the hybrid structure can make a very high energy density in the sandwiched low refractive index layer.

Acknowledgements This work was supported partially by the National Natural Science Foundation of China (Grant Nos. 61178062 and 61108022).

References

1. Ozbay E. Plasmonics: merging photonics and electronics at nanoscale dimensions. Science, 2006, 311(5758): 189–193
2. Zia R, Schuller J A, Chandran A, Brongersma M L. Plasmonics: the next chip-scale technology. Materials Today, 2006, 9(7–8): 20–27
3. Tanaka K, Tanaka M. Simulations of nanometric optical circuits based on surface plasmon polariton gap waveguide. Applied Physics Letters, 2003, 82(8): 1158–1160
4. Kusunoki F, Yotsuya T, Takahara J, Kobayashi T. Propagation properties of guided waves in index-guided two-dimensional optical waveguides. Applied Physics Letters, 2005, 86(21): 211101
5. Pile D F P, Gramotnev D K. Plasmonic subwavelength waveguides: next to zero losses at sharp bends. Optics Letters, 2005, 30(10): 1186–1188
6. Liu L, Han Z H, He S. Novel surface plasmon waveguide for high integration. Optics Express, 2005, 13(17): 6645–6650
7. Veronis G, Fan S H. Bends and splitters in metal-dielectric-metal subwavelength plasmonic waveguides. Applied Physics Letters, 2005, 87(13): 131102
8. Pile D F P, Gramotnev D K. Channel plasmon-polariton in a triangular groove on a metal surface. Optics Letters, 2004, 29(10): 1069–1071
9. Bozhevolnyi S I, Volkov V S, Devaux E, Laluet J Y, Ebbesen T W. Channel plasmon subwavelength waveguide components including interferometers and ring resonators. Nature, 2006, 440(7083): 508–511
10. Oulton R F, Sorger V J, Genov D A, Pile D F P, Zhang X. A hybrid plasmonic waveguide for subwavelength confinement and long-range propagation. Nature Photonics, 2008, 2(8): 496–500
11. Fujii M, Leuthold J, Freude W. Dispersion relation and loss of subwavelength confined mode of metal-dielectric-gap optical waveguides. IEEE Photonics Technology Letters, 2009, 21(6): 362–364
12. Dai D X, Yang L, He S L. Ultrasmall thermally tunable microring resonator with a submicrometer heater on Si nanowires. Journal of Lightwave Technology, 2008, 26(6): 704–709
13. Alam M Z, Meier J, Aitchison J S, Mojahedi M. Propagation

characteristics of hybrid modes supported by metal-low-high index waveguides and bends. Optics Express, 2010, 18(12): 12971–12979
14. Dai D X, He S L. A silicon-based hybrid plasmonic waveguide with a metal cap for a nano-scale light confinement. Optics Express, 2009, 17(19): 16646–16653
15. Dai D X, Shi Y C, He S L, Wosinski L, Thylen L. Gain enhancement in a hybrid plasmonic nano-waveguide with a low-index or high-index gain medium. Optics Express, 2011, 19(14): 12925–12936
16. Ordal M A, Bell R J, Alexander R W Jr, Long L L, Querry M R. Optical properties of fourteen metals in the infrared and far infrared: Al, Co, Cu, Au, Fe, Pb, Mo, Ni, Pd, Pt, Ag, Ti, V, and W. Applied Optics, 1985, 24(24): 4493–4499